Supplemental Information

A. Comparison of magnitude-based and combined complex and magnitude-based separation methods for FF quantification in the supraclavicular fat depot.

In 5 subjects (L, M, N, O, and P) FF maps were obtained by using the magnitude-based water-fat separation algorithm (as described in the paper), as well as by using a combined magnitude-based and complex-based water-fat separation algorithm, as described in Yu et al., to assess difference in fat fraction quantification between these two methods.(29)

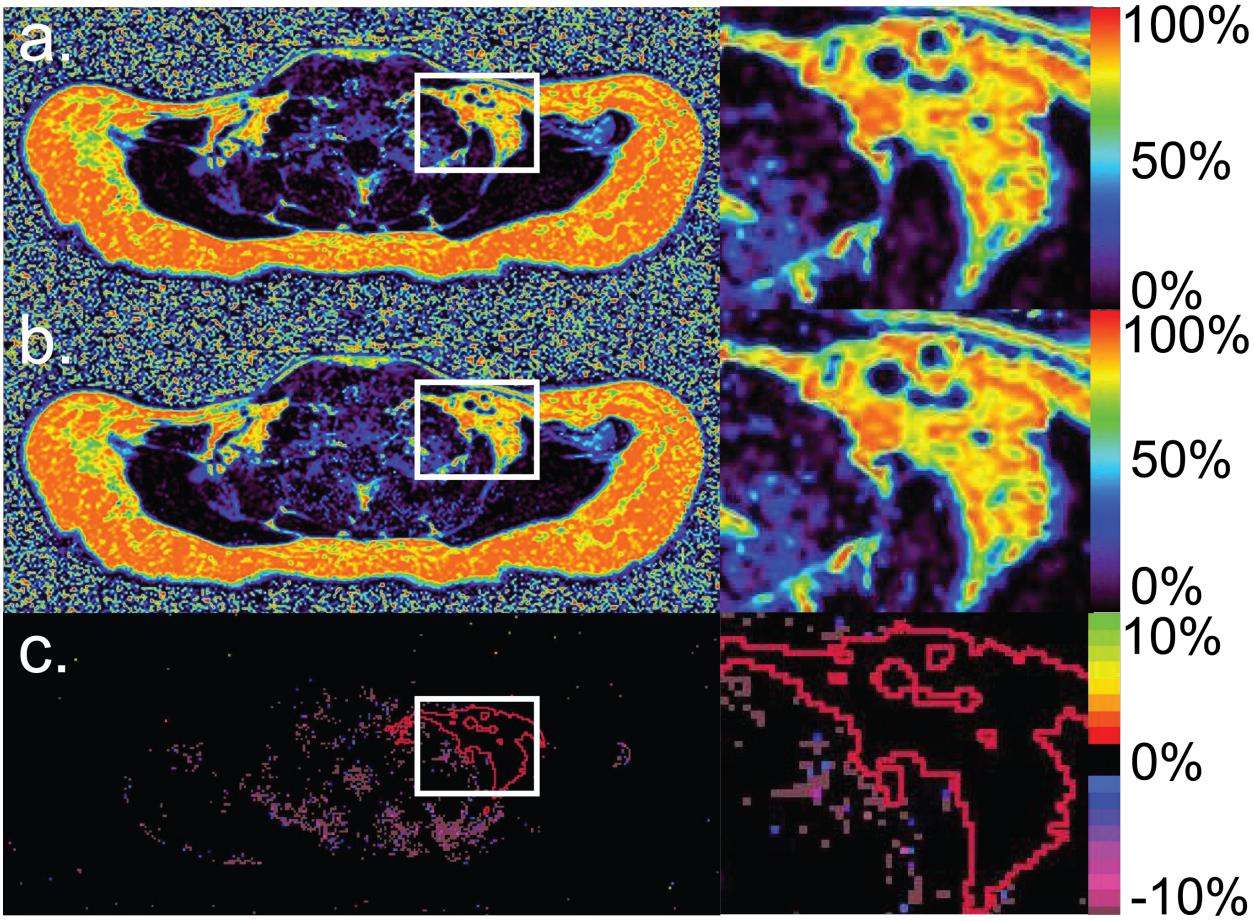

Supporting Figure S1. Example of FF maps obtained with different FF separation algorithms for an axial slice encompassing the supraclavicular fat depot from subject P. a. FF map obtained by using the magnitude-based algorithm b. FF map obtained by using the combined magnitude-based and complex-based separation algorithm. c. Difference map. Right side shows the supraclavicular fat depot with the region corresponding to BAT_{MRI} (FF>40%) outlined in red. No differences in FF were observed within the supraclavicular fat depot.

As is shown in Figure S1, FF values obtained with the two reconstruction algorithms are the same in the supraclavicular fat region, identified as BAT_{MRI} (FF > 40), in all 5 subjects analyzed. On the other hand, differences were found in regions with a FF of about 30%, mainly at boundaries between different tissues and at boundaries between tissue and blood vessels.

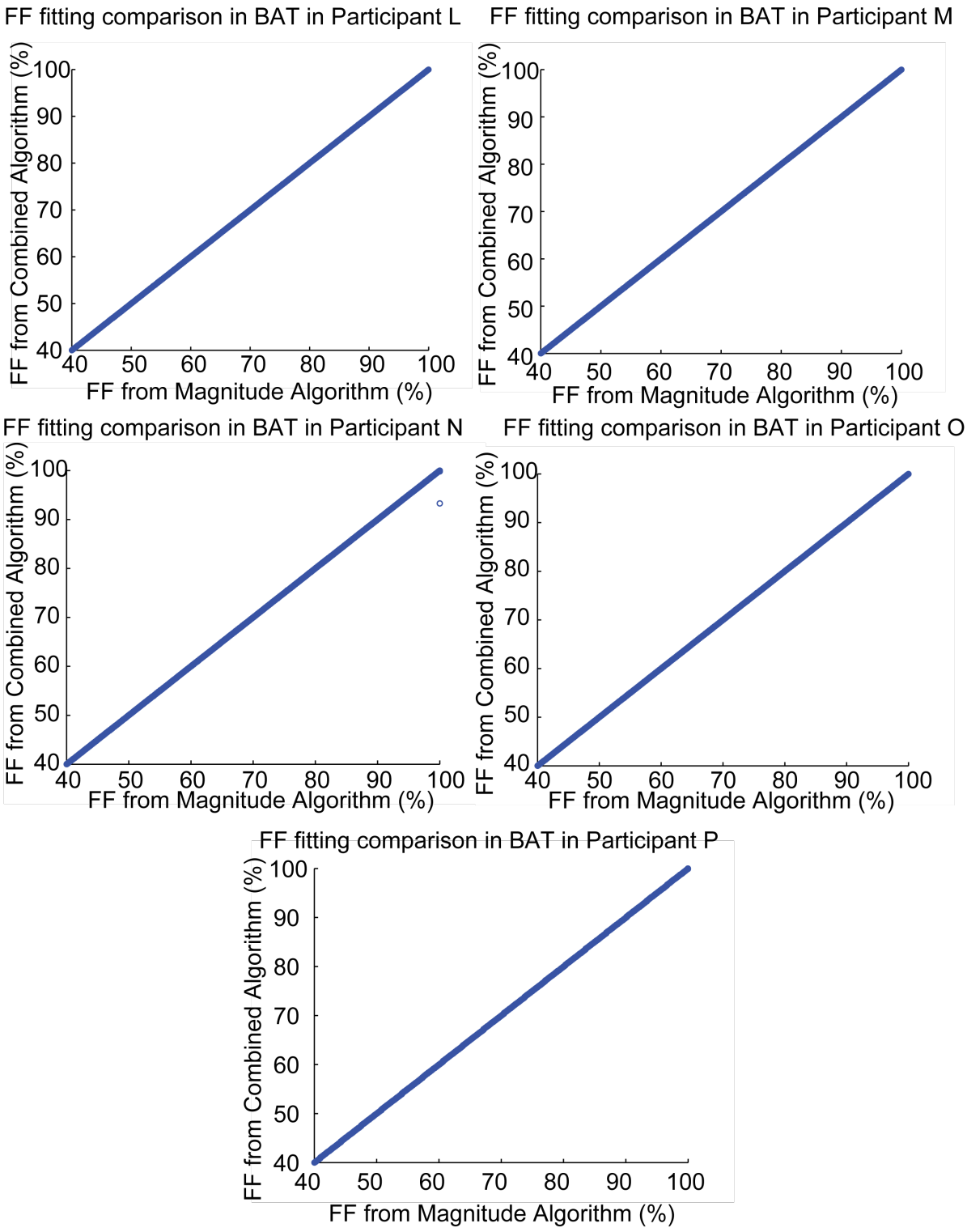

Supporting Figure S2. Plots showing FF values obtained with the two different algorithms for each voxel within the supraclavicular fat depot identified as BAT_{MRI} (FF>40%). For all 5 subjects, the same FF values were obtained by using the two algorithms (linear trend with a R^2=1, slope=1, and y int.<10^{-11}).

Despite the combination of complex-based and magnitude-based separation methods having been shown to be more accurate than magnitude-based separation methods for FF quantification in general, in those regions of the supraclavicular depot idenitified as BAT_{MRI} (FF>40%) the two methods gave the same FF values.

B. R2* and FF plotted against SUV for all subjects analyzed.

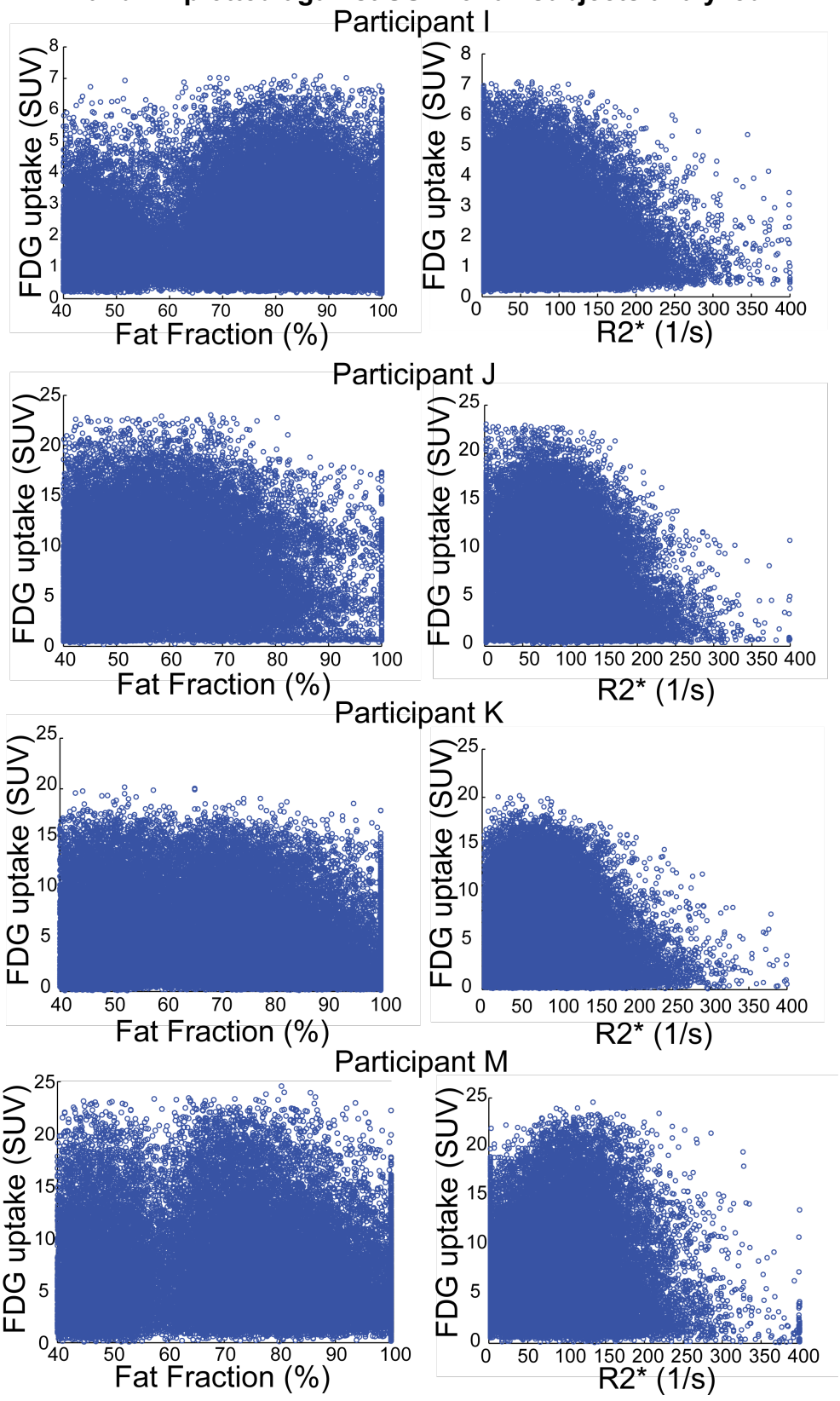

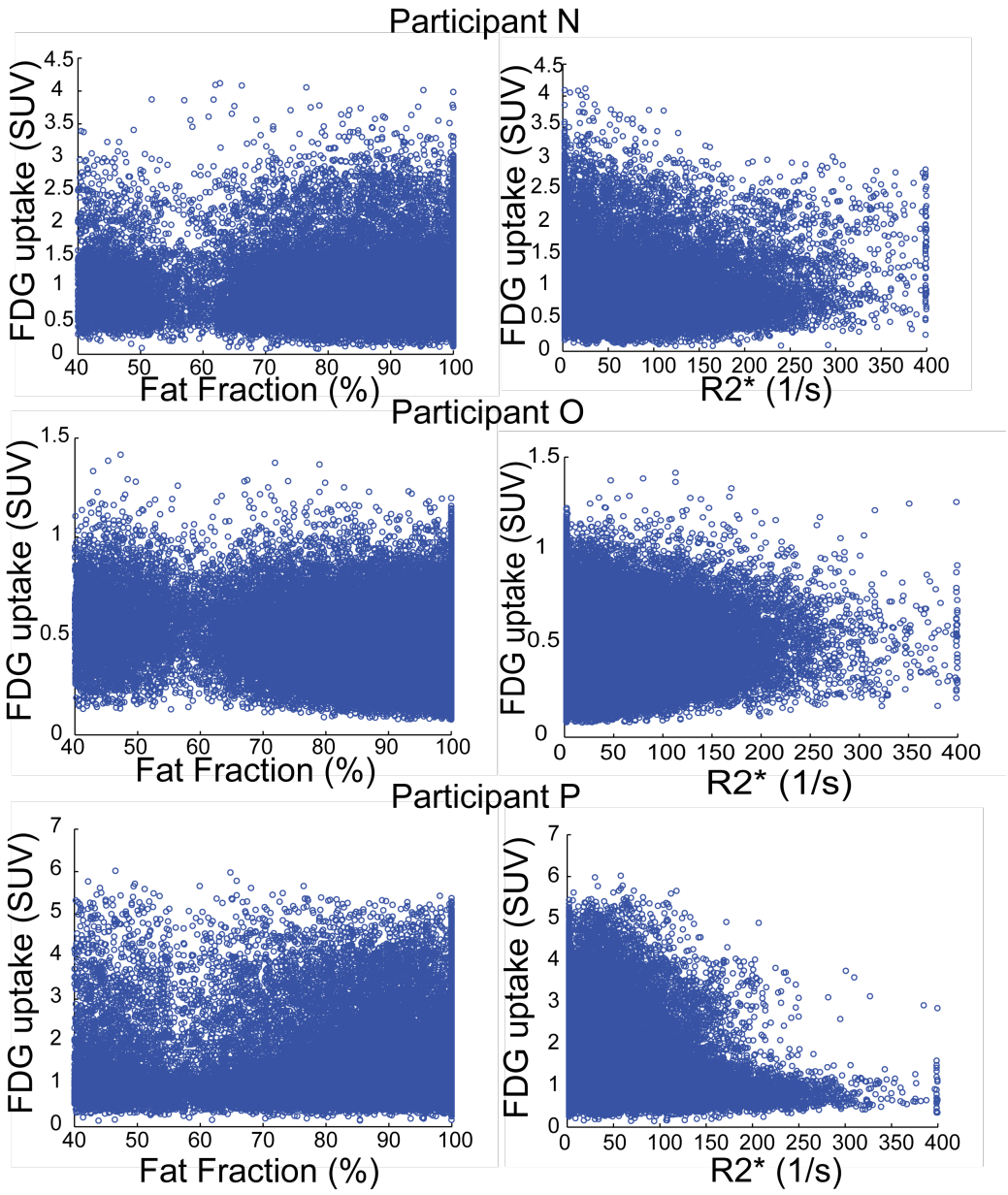

Supporting Figure S3. Plots of FDG uptake vs. FF and R2* for all voxels identified as BAT_{MRI} (FF>40) for seven participants. A linear regression analysis was run on both plots as well as on both the R2* and FF data together allowing for quadratic and interaction terms. R^2 values are given for each fit. No clear, general trend was observed between FF or R2* and glucose uptake in any of the subjects. Participant I, R^2: FF=0.013 R2*=0.006 Combination=0.04. Participant J, R^2: FF=0.002 R2*=0.026 Combination=0.04. Participant K, R^2: FF=0.020 R2*=0.025 Combination=0.068. Participant M, R^2: FF=0.0001 R2*=0.020 Combination= 0.040. Participant N, R^2: FF=0.002 R2*=0.0001 Combination=0.079. Participant O, R^2: FF=0.053 R2*=0.014 Combination=0.057. Participant P, R^2: FF=0.001 R2*=0.011 Combination=0.029.

C. Average FF value of $BAT_{PET/MRI}$ plotted vs. time during cold exposure for FDG positive participants.

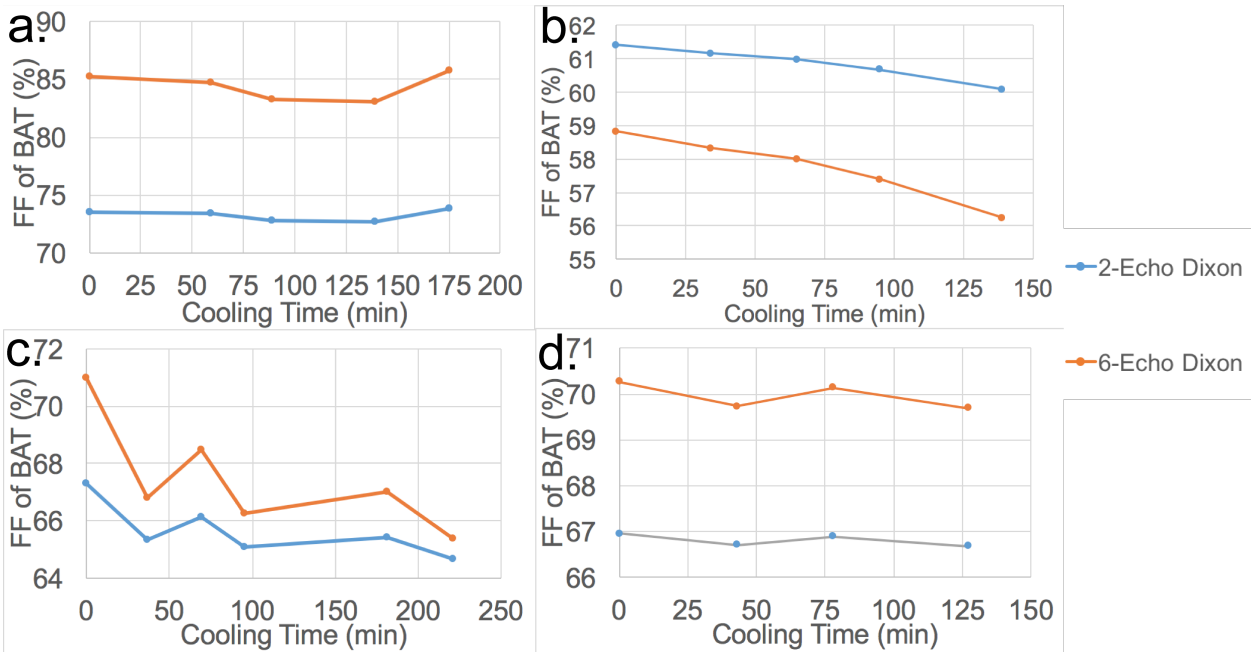

Supporting Figure S4. Average FF values for the $BAT_{PET/MRI}$ volume identified in subjects C, E, F, and G measured during cold exposure. Subjects E and F (b. and c.) showed a decrease in the average BAT fat fraction value during the individualized cooling protocol while participants C and G (a. and d.) did not.